Anal. Chem. **XXXX,** *xxx,* 000–000

Measuring Surface Charge Density and Particle Height Using Surface Plasmon Resonance Technique

Xiaonan Shan,[†] Xinping Huang,[†] Kyle J. Foley,[†] Peiming Zhang,[†] Kangping Chen,[‡] Shaopeng Wang,[†] and Nongjian Tao*[,†]

Department of Electrical Engineering, Center for Bioelectronics and Biosensors, Biodesign Institute, and Department of Aerospace/Mechanical Engineering, Arizona State University, Tempe, Arizona 85287-5801

We demonstrate a method to measure surface charge density and particle height using surface plasmon resonance (SPR) detection. It is based on two facts: (1) The equilibrium height of a charged particle over a charged surface depends on the electrostatic interaction between the particle and the surface; and (2) SPR is extremely sensitive to the height of the particle. We perform numerical simulations to establish the relations between the SPR signal and the particle height, and between the particle height and the surface charge density, and carry out systematic experiments, including effects of different buffer concentrations, particle sizes, and concentrations, to examine the relations. The simulation and experimental results are in good agreement with each other. Using the method, we determine surface charge density of gold surface functionalized with different molecules. If the surface charge density is known, the method can also be used to determine the charges of the particles.

Surface charge density is a fundamentally important quantity, and measuring it has a broad impact on many applications. For example, electrostatic charge on sensor surfaces has profound effects on DNA hybridization and protein binding in microarray technologies.[1] Quantification of surface charge density can lead to a better understanding of biomolecular interactions on surfaces. In addition, measurement of surface charge density can be used as a signal transduction mechanism to detect molecular binding events on surfaces.[2] Several methods have been developed to measure surface charge density. One is potentiometric titration, which is limited to measuring the average charge density of an entire surface.[3,4] Atomic force microscopy can probe local charge density with high resolution,[5,6] but it is slow and can cover only a small sample area.[7,8] A reflection interference contrast microscope has also been used to measure the surface charge density,[2,9] but it requires well-defined, smooth, and spherical particles to obtain well-defined interference patterns.

Here, we report on a surface plasmon resonance (SPR) method to measure surface charge density. As compared to the previously reported methods, the SPR approach has the following distinct features: (1) It offers spatial resolution (submicrometer resolution[10]) when operated in the imaging SPR mode, which is ideal for high throughput mapping of heterogeneous surface charge distribution. (2) SPR can measure the local coverage of molecules, making it possible to study the correlation between the coverage and surface charge density. (3) It allows one to monitor various surface processes, including molecular binding, on the same surface after determination of surface charge density. (4) It can be used to measure the charge density of not only surfaces but also the particles, including cells. (5) Finally, the approach may be used to study the interactions between the particles and surfaces.

SPR is extremely sensitive to refractive index changes near a metal film (sensor surface), which has been used as real-time and label-free technique for many applications, ranging from environmental studies to biomedical research. Most SPR applications, to date, are based on the detection of molecular binding on sensor surfaces.[11] Because the evanescent field associated with SPR penetrates into the solution phase over a distance of ~200 nm, SPR probes refractive index changes within the entire penetration depth. The intensity of the evanescent field decays exponentially, making SPR also an extremely sensitive tool to measure the distance between an object and the sensor surface. The object could be macromolecules, cells, nanoparticles, or glass beads, so long as its index of refraction is different from that of the liquid medium. In this work, we demonstrate that this sensitive distance dependence can be used to determine the surface charge density and particle height.

* To whom correspondence should be addressed. Phone: 480-965-4456. Fax: 480-965-9457. E-mail: njtao@asu.edu.

[†] Department of Electrical Engineering, Center for Bioelectronics and Biosensors, Biodesign Institute.

[‡] Department of Aerospace/Mechanical Engineering.

(1) Heaton, R. J.; Peterson, A. W.; Georgiadis, R. M. *Proc. Natl. Acad. Sci. U.S.A.* **2001**, *98*, 3701–3704.
(2) Clack, N. G.; Salaita, K.; Groves, J. T. *Nat. Biotechnol.* **2008**, *26*, 825–830.
(3) Sanchez, J.; del Valle, M. *Crit. Rev. Anal. Chem.* **2005**, *35*, 15–29.
(4) Gibson, G. T. T.; Mohamed, M. F.; Neverov, A. A.; Brown, R. S. *Inorg. Chem.* **2006**, *45*, 7891–7902.
(5) Xu, S. H.; Arnsdorf, M. F. *Proc. Natl. Acad. Sci. U.S.A.* **1995**, *92*, 10384–10388.
(6) Campbell, S. D.; Hillier, A. C. *Langmuir* **1999**, *15*, 891–899.
(7) Sinensky, A. K.; Belcher, A. M. *Nat. Nanotechnol.* **2007**, *2*, 653–659.
(8) Butt, H. J.; Cappella, B.; Kappl, M. *Surf. Sci. Rep.* **2005**, *59*, 1–152.
(9) Clack, N. G.; Groves, J. T. *Langmuir* **2005**, *21*, 6430–6435.
(10) Berger, C. E. H.; Kooyman, R. P. H.; Greve, J. *Rev. Sci. Instrum.* **1994**, *65*, 2829–2836.
(11) Hoa, X. D.; Kirk, A. G.; Tabrizian, M. *Biosens. Bioelectron.* **2007**, *23*, 151–160.

10.1021/ac901816z

Scheme 1. Schematic Illustration of the Surface Charge Density Detection Principle

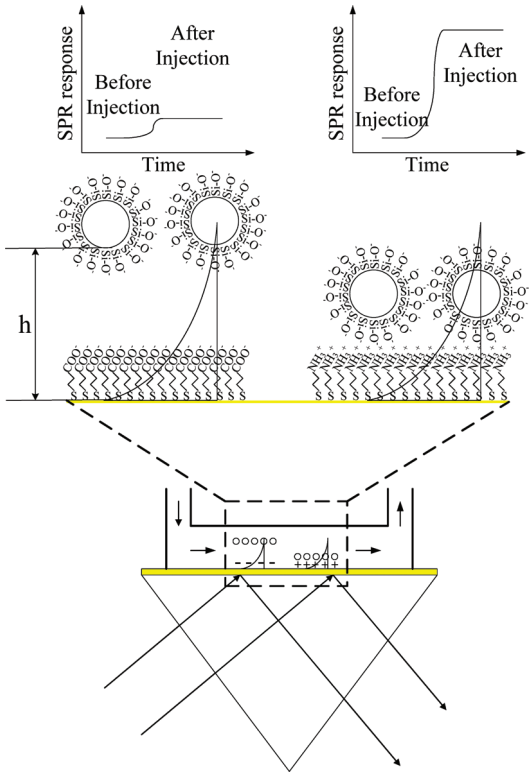

THEORY

Scheme 1 illustrates the basic principle of the method, in which charged silica particles are used as probes to measure the surface charge density of a sensor chip. If the silica particle probes have the same charge as the sensor surface, then the electrostatic repulsion will prevent the particles from reaching the surface. The equilibrium height of a silica particle from the surface depends on the electrostatic force between the particle and the surface. Because the equilibrium height can be accurately measured with SPR, one can thus determine the surface charge density.

A quantitative relation between surface charge density and the particle height can be derived on the basis of the balance between two forces, electrostatic repulsion that tends to drive the particles away from the surface and the gravitational force that moves the particles toward the surface. As shown in the Supporting Information, the surface charge density is given in terms of the particle height, h, by[9,12−17]

$$\sigma = \frac{2\varepsilon\varepsilon_0 k_B T\kappa}{e}\sinh\left(\frac{2\tanh^{-1}(\zeta \cdot e^{\kappa h})}{2k_B T}\right) \quad (1)$$

where ε is the relative permittivity of water, ε_0 is the vacuum permittivity, k_B is the Boltzmann constant, T is the temperature, e is the electron charge, κ^{-1} is the Debye length, and h is the particle height measured the bottom of the particle to the surface. ζ in eq 1 is given by

$$\zeta = \frac{\kappa^{-1}F_g}{64\pi\varepsilon\varepsilon_0 R\left(\frac{k_B T}{e}\right)^2 \tanh\left(\frac{e\psi_p}{4k_B T}\right)} \quad (2)$$

where R and ψ_p are the radius and surface potential of the particle, respectively. F_g in eq 2 is net gravitational force on the particle, which is

$$F_g = \frac{4\pi}{3}R^3(\rho_p - \rho_f)g \quad (3)$$

where g (= 9.8 m/s^2) is the free fall acceleration, and ρ_p and ρ_f are the mass densities of the particle and fluid, respectively. For silica particles and aqueous fluid with moderate salt concentrations, $\rho_p = 2 \times 10^3$ kg/m^3 and $\rho_f = 10^3$ kg/m^3. Using eq 1, together with eqs 2 and 3, we plot the surface charge density, σ, as a function of the distance, h (Figure 1a). The plot shows that the logarithmic surface charge density is approximately

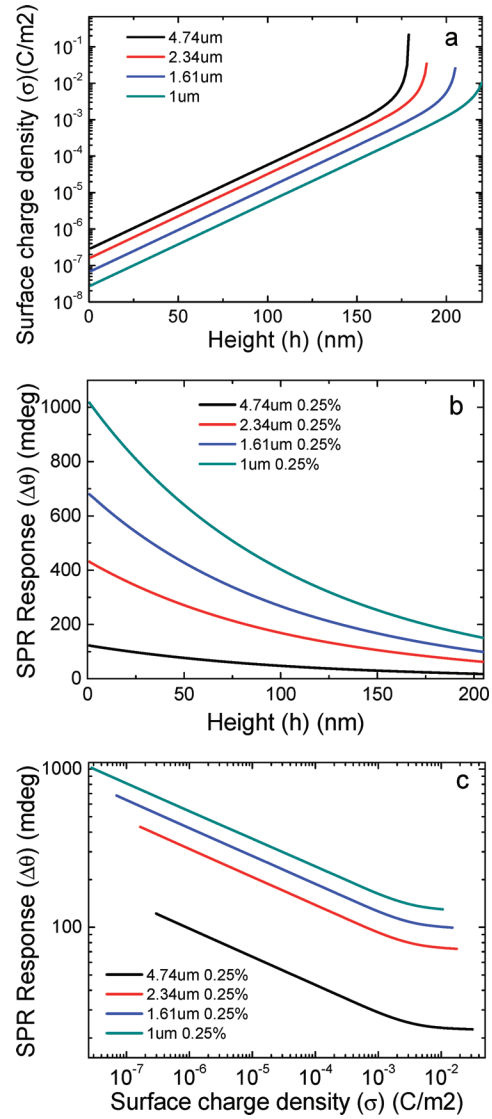

Figure 1. (a) Surface charge density versus particle equilibrium height. (b) SPR response versus particle equilibrium height. (c) SPR response versus surface charge density.

(12) Behrens, S. H.; Grier, D. G. *J. Chem. Phys.* **2001**, *115*, 6716–6721.
(13) Wu, H. J.; Pangburn, T. O.; Beckham, R. E.; Bevan, M. A. *Langmuir* **2005**, *21*, 9879–9888.
(14) Wu, H. J.; Bevan, M. A. *Langmuir* **2005**, *21*, 1244–1254.
(15) Frej, N. A.; Prieve, D. C. *J. Chem. Phys.* **1993**, *98*, 7552–7564.
(16) Hsu, J. P.; Liu, B. T. *J. Chem. Phys.* **1999**, *110*, 25–33.

proportional to the particle height. Once the equilibrium height is known, we can then determine the surface charge density using the relation.

As we have mentioned already, the equilibrium height of the particles can be measured using SPR. We have performed numerical calculations[18,19] of the dependence of the SPR angular shift versus the height for silica particles with different diameters (Figure 1b). The details of the model and simulation procedures are described in the Supporting Information. The simulation shows that the SPR response decreases rapidly with the height, due to the exponential decay of the evanescence field from the surface into the fluid phase. Combining Figure 1a and b, the relation between the SPR response and surface charge density is plotted in Figure 1c. It shows that within a broad range of surface charge density, the logarithm of the SPR angular shift decreases linearly with the logarithm of the surface charge density, which can be readily used to determine the surface charge density on the basis of measured SPR angular shift.

As shown in Figure 1c, the relation between the SPR response and the surface charge density depends on the particle size. For a given change in the surface charge density, smaller particles produce larger SPR responses. This observation can be understood on the basis of geometrical considerations (see Figure S1 and Particle Size Effect in the Supporting Information). However, if the particle is too small, then Brownian motion becomes important, and a more complete theory including thermal fluctuations will be needed. Exploring this regime is of great interest and will be a subject of future studies. Brownian motion becomes important when the gravitational energy, $(4\pi)/(3)r^3(\rho_p - \rho_f)gh$, reduces to the same level as the thermal energy, k_BT, or $(4\pi)/(3)r^3(\rho_p - \rho_f)gh \approx k_BT$. Assuming $h \approx 200$ nm, we found that the radius of the particle is about 0.7 μm.

Another approximation made in deriving eqs 1−3 is the negligence of the van der Waals interaction between the particles and the surface. The van der Waals force between a silica particle and a flat surface is given by $F_{vdw} = AR/h$, where A is the Hamaker constant.[20] For water, $A = 1.5 \times 10^{-19}$ J, and the van der Waals force for a 1 μm diameter particle in contact with the surface is $\sim 10^{-17}$ N, which is several orders of magnitude smaller than the gravitational force, $(4\pi)/(3)r^3(\rho_p - \rho_f)g \approx 10^{-14}$ N. This analysis justifies the approximation of neglecting the van der Waals interaction.

In a previous publication,[21] we have described a different SPR method to determine surface charge and impedance. The method relies on the dependence of SPR frequency on the surface charge density, which leads to a surface-charge-dependent SPR angular shift given by $\Delta\theta_R = \beta\Delta\sigma$, where $\Delta\theta_R$ is the SPR angular shift and $\Delta\sigma$ is the surface charge change (where the β describes the sensitivity). The sensitivity, β, was found to be 0.021 deg/C/m^2.[21] In contrast, the sensitivity of the present method is 1 deg/C/m^2 for an equilibrium height of 200 nm, which is 2 orders of magnitude more sensitive than the direct method. If decreasing the height to zero, the sensitivity increases to 10^6 deg/C/m^2.

EXPERIMENTAL SECTION

Reagents and Chemicals. HPLC-grade 3-mercaptopropionic acid (3-MPA), cysteamine hydrochloride, sodium chloride, and sodium acetate anhydrous were purchased from Sigma-Aldrich (St. Louis, MO). 3-MPA and cysteamine hydrochloride were used as received. Glacial acetic acid was supplied by Mallinckrodt chemicals (Philipsburg, NJ). Phosphate buffer saline (PBS) tablet was purchased from Calbiochem (Darmstadt, Germany). Silica particles, with diameters of 1.00, 1.61, 2.34, and 4.74 μm, were purchased from Bangs Laboratories (Fishers, IN). Zeta potentials of the silica particles were measured using Zetasizer Nano (Malvern Instruments, Worcestershire, UK). Ultrapure water (18.2 MΩ cm) from ELGA was used for preparing all of the solutions.

SPR Setup. BI-2000 SPR system (Biosensing Instrument, Tempe, AZ, www.biosensingusa.com) was used for SPR measurements. The wavelength of the incident light is 635 nm. The system is equipped with a flow cell made of a PEEK (polyaryletheretherketone) cell block and a PDMS (polydimethylsiloxane) gasket containing two channels. It has a valve control system that can switch the flow between single channel mode and serial channel mode. In the single channel mode, a sample solution injected via an injection valve flows through either channel 1 or channel 2, while in the serial channel mode the sample flows through the two channels sequentially. Before each experiment, the flow cell was cleaned with ethanol and DI water. The SPR sensor chip was a BK7 glass cover slide coated with 1.5 nm chromium followed by 47 nm gold by thermal evaporator at high vacuum (3×10^{-6} Torr).

Surface Modification. Before each experiment, a gold sensor chip was rinsed with ethanol and deionized water and then annealed with a hydrogen flame to remove possible surface contamination. The chip was modified using the flow-through system of the SPR instrument. For example, 10 mM 3-MPA was injected into channel 1 to create a negatively charged surface, and 10 mM cysteamine hydrochloride was injected into channel 2 to create a positively charged surface using the single channel mode. The surface modification processes were monitored with the SPR in real time. As the molecules bound to the gold surface, the SPR signal increased and eventually reached a steady value, indicating the formation of a full monolayer coverage. All experiments were carried out using a flow rate of 60 μL/min.

Buffer System and Silica Particle Solution Preparation. Different solutions, including acetate buffer and NaCl solutions, were used as running buffers. NaCl solutions with concentrations varying from 0.1 to 10 mM were used to test the electrical double layer screening effect. The acetate buffer was prepared by mixing of 37 mM sodium acetate anhydrous and 10 mM glacial acetic acid, which was diluted to 2, 1, 0.5, 0.25, and 0.1 mM. All of the buffers were used immediately after preparation to minimize possible contamination.

The silica particle sample received from the vendor contained 10% (by mass ratio) silica particles suspended in deionized water. Before each experiment, the sample was rinsed five times with deionized water and extracted by centrifuge after each rinsing step. Different amounts of silica particles were then added into the acetate buffers to reach final particle concentrations at 0.0625%,

(17) Liang, Y.; Hilal, N.; Langston, P.; Starov, V. *Adv. Colloid Interface Sci.* **2007**, *134−35*, 151–166.
(18) Shan, X. N.; Foley, K. J.; Tao, N. J. *Appl. Phys. Lett.* **2008**, *92*, 133901.
(19) Hansen, W. N. *J. Opt. Soc. Am.* **1968**, *58*, 380–390.
(20) Israelachvili, J. N. *Intermolecular and Surface Forces*, 2nd ed.; Academic Press: New York, 1991.

0.125%, 0.25%, 0.5%, and 1%. The zeta potentials of the silica particles were determined to confirm the surface charges of the particles (see the Supporting Information).

RESULTS AND DISCUSSION

Ionic Strength Effect. One of the key assumptions in deriving eq 1 is that the electrostatic force between the particle and surface is determined by the Poisson−Boltzmann equation. An important prediction of the Poisson−Boltzmann equation is that the electrostatic force depends on the ionic concentration via the Debye length, κ^{-1}, which measures the screening length of the electrostatic force by the ions. For monovalent ions, $\kappa^{-1} \approx 0.3$ nm/$\sqrt{(c[\mathrm{M}])}$, where c is the ionic concentration in molarity, showing that the Debye length decreases with the ionic concentration. To verify the theory, we measured the particle height as a function of ionic concentration (0.1−10 mM NaCl solution). We note that the change in the ionic concentration also causes a change in the solution pH from 6.2 to 6.0, but the pH change is small and not expected to change the electrostatic force between the particle and the surface.

Figure 2a shows the SPR response (blue curve) of 0.25% 2.34 μm diameter silica particles as a function of NaCl concentration. The sensor surface was modified with 3-MPA monolayer, so the balance between the electrostatic repulsion and gravity determines the equilibrium height. Using the relation shown in Figure 1b, we determined the particle height versus NaCl concentration (black curve, Figure 2a). As expected, the equilibrium height decreases with the ionic concentration. We fitted the experimental data using eq 1 with fitting parameters, $\sigma = -2$ mC/m^2 and $\Psi_p = -31$ mV. The fit is excellent, and the fitting parameter σ matches closely with the independently measured values (we will return to this later). The second fitting parameter, $\Psi_p = -31$ mV, is also in close agreement with the independently measured[22] and calculated values (−30.5 mV) reported in the literature.[12] The quantitative agreement between the experimental data and theoretical prediction supports the simple theory described in the principle section. Note that the variation in the NaCl concentration also introduces a change in the refractive index of the medium. We measured the angle shift due to different NaCl concentrations before each experiment, which was found to be relatively small (<11 mdeg), and subtracted it out from the total signal.

Particle Size Effect. The theory described in the Theory section also predicts that smaller particles produce greater changes in the SPR responses than the larger particles, thus leading to more sensitive detection of surface charge density (see Figure 1c). This is because the smaller particles have larger interaction volumes within the evanescent field near the SPR sensor surface. To verify the prediction, we measured SPR responses to silica particles with various diameters. Because the SPR response depends on not only the size but also the coverage of the particles, we ensured a complete coverage of the sensor surface with the particles in each experiment. This was achieved by (1) using sufficiently concentrated particle solutions and (2) modifying the surface with cysteamine·HCl to create a positively charged surface that attracted the particles onto the surface.

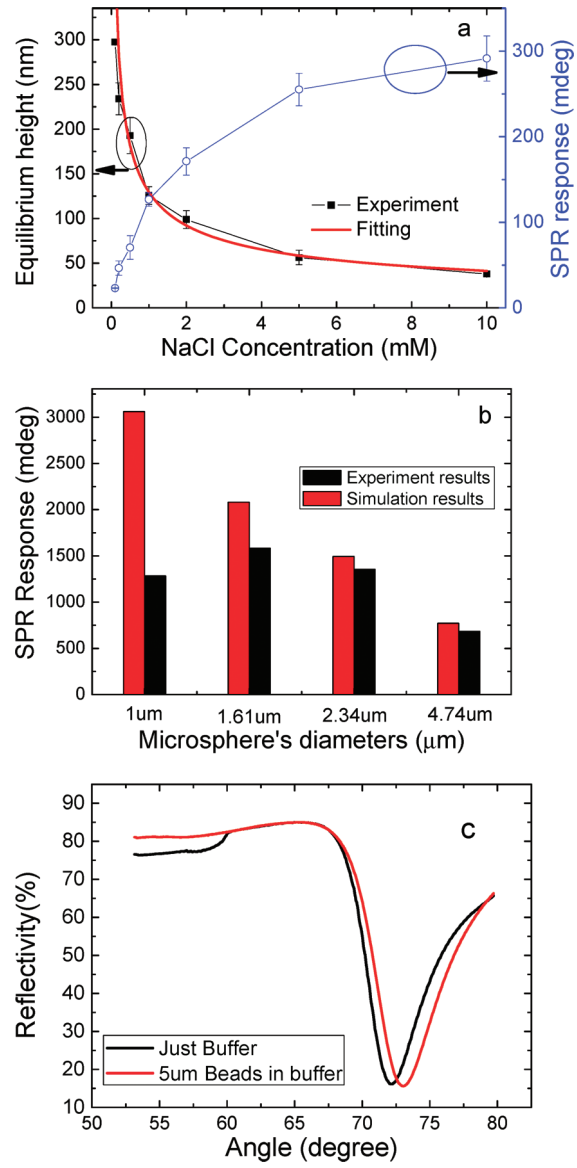

Figure 2. (a) Experimental (■) and theoretical (red line) equilibrium heights versus NaCl concentration. The 2.34 μm 0.25% silica particle was used for measurements. The SPR response versus NaCl concentration was also plotted. (b) Experimental and theoretical SPR responses for particles with different diameters. (c) Measured SPR profiles with (red curve) and without (black curve) the presence of full monolayer 5 μm silica beads in 0.5 mM acetate buffer.

We also carried out numerical simulation of the SPR response versus particle size using procedures described in the Supporting Information. Note that the distance between Au surface and particle was set at 1 nm to represent the thickness of cysteamine·HCl monolayer. Both the experimental and the simulated SPR responses versus particle size are shown in Figure 2b. For 4.74 and 2.34 μm diameter particles, the simulation and experiment are in good agreement. The small errors between simulation and experiment results come from the imperfect monolayer coverage. Deviations between the simulated and measured SPR responses begin to appear for the 1.61 and 1 μm diameter particles. While the dynamic range of the SPR setup may affect the result for the small particles, the Brownian motion effect is expected to play an increasing role as the particles decrease in size. The estimated

(21) Foley, K. J.; Shan, X.; Tao, N. J. *Anal. Chem.* **2008**, *80*, 5146–5151.

critical size, below which Brownian motion becomes non-negligible, is ~1.4 μm. This value is consistent with the observation shown in Figure 2b. It is important to note that although eq 1 will no longer hold when Brownian motion becomes important, the method of measuring surface charge density on the basis of SPR should still work as long as the electrostatic force affects the distribution of the particles near a charged surface.

The presence of particles on the surface may introduce scattering to the evanescent field, which would increase the intensity at resonance and distort the SPR profile. We have measured SPR profiles (reflection versus angle) in the presence and absence of a full monolayer of 5 μm particles. Here, the full monolayer corresponds to the formation of a closely pack layer of particles on the surface, which is confirmed directly with an optical microscope and indirectly on the basis of the saturation in the SPR angular shift. As shown in Figure 2c, the SPR profile in the presence of particles remains well-defined, and the intensity at the resonant angle remains unchanged as compared to the profile measured without the particles. We have also simulated SPR by representing the particles with a homogeneous layer with refractive index calculated from the particle packing density and refractive indices of water and the silica particles, and we found that the measured shift in the resonant angle due to the presence of the particles is in good agreement with the calculated angular shift (Supporting Information). These observations indicate that the scattering is relatively small for the purpose of the present project.

Positive and Negative Charged Surfaces. To demonstrate the principle of the method, we measured the SPR responses using negative and positive surfaces. First, channel 1 and channel 2 were modified with 10 mM 3-MPA and 10 mM cysteamine·HCl solution by operating the fluidics in the single mode to create negatively and positively charged surfaces (in 0.5 mM acetate buffer) independently. After surface modification, the fluidics was switched to serial mode, and silica particle solution was flown through the two channels sequentially for 1 min. The pump was then stopped to allow the particles to redistribute and settle on the negatively and positively charged surfaces in channels 1 and 2. After the SPR signals reached steady states, indicating that the particles approached equilibrium, acetate buffer was introduced to flush out the remaining particles suspended in the solution. Finally, the surfaces of both channels were regenerated with 10 mM NaOH.

Figure 3 shows the SPR response of a complete experimental cycle, including injection and redistribution of the silica particles, flushing out the unsettled particles, and surface regeneration. Immediately after injecting 100 μL of the silica particles solution into the cell, the SPR signals of both channels 1 and 2 increased slightly (marked by "1"). Most particles at this point were still suspended in the solution. The pump was turned off to allow the suspended particles to settle on the surfaces, which was shown by the steady increases in the SPR responses ("2"). Within 1−2 min, the particles reached equilibrium. For the negatively charged surface (channel 1), the corresponding steady-state SPR signal is about 67 mdeg. In contrast, the SPR response reached 635 mdeg, nearly 10 folds greater, for the positively charged surface in channel 2. The large difference can be easily understood because the negatively charged particles were repelled from the negatively charged surface in channel 1 and attracted to the positively charged surface in channel 2.

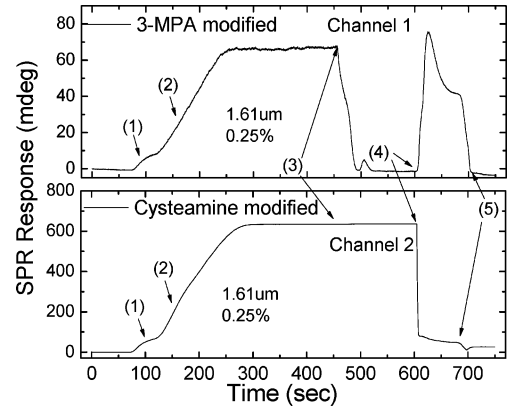

Figure 3. SPR response of negatively charged surface (modified with 3-MPA) and positively charged surface (modified with cysteamine·HCl) during different stages including (1) sample injection, (2) particle redistribution, (3) flushing, (4) surface regeneration, and (5) returning to baseline. 1.61 μm diameter silica particles in 0.5 mM acetate buffer with volume concentration of 0.25% were used in the experiments.

The two channels also responded differently during the flushing stage ("3"), which was supposed to remove the suspended particles out of the fluidic channels with the running buffer. In channel 1, due to the repulsive force, most particles were suspended, which were completely flushed out, and the corresponding SPR signal returned to the original baseline. However, in channel 2, the SPR response did not change much. This is also expected because a complete layer of silica particles was attracted onto the surface, which could not be easily flushed out of the channel. To remove the particles from the surface in channel 2, we introduced 10 mM NaOH into the cell ("4"), which neutralized the surface and allowed us to flush the particles out of the channel. As a result, the SPR signal returned to the original baseline ("5"). The spikes in the channel 1 signal after the injection of NaOH were due to the particles released from channel 2 flushing through the channel 1. These experiments established the basic principle for the determining surface charge density using SPR. We note that the surfaces of both channels 1 and 2 were regenerated by the 10 mM NaOH injection, allowing us to reuse the chip.

Particle Concentration Effect. The experiment discussed above demonstrated the detection of surface charges using 1.61 μm particles at 0.25%. However, as we have discussed in the principle section, the detection sensitivity depends on the concentration of the particles. We have shown that smaller particles give better sensitivity, but if the particles are too small then Brownian motion becomes important, which decreases the residence time of the particles on the surface and thus leads to smaller SPR responses.We have examined the particle concentration effect on the sensitivity by comparing the SPR responses of 1, 1.61, 2.34, and 4.74 μm diameter particles at different particle concentrations. Figure 4a shows the SPR responses of 1.61 and 2.34 μm particles exposed to 3-MPA- and cysteamine·HCl-modified surfaces at five different particle concentrations. Following each injection of the particles into the fluidic channels, the surface was regenerated with 10 mM NaOH, which led to a spike in the SPR signal. From the SPR response curves, we

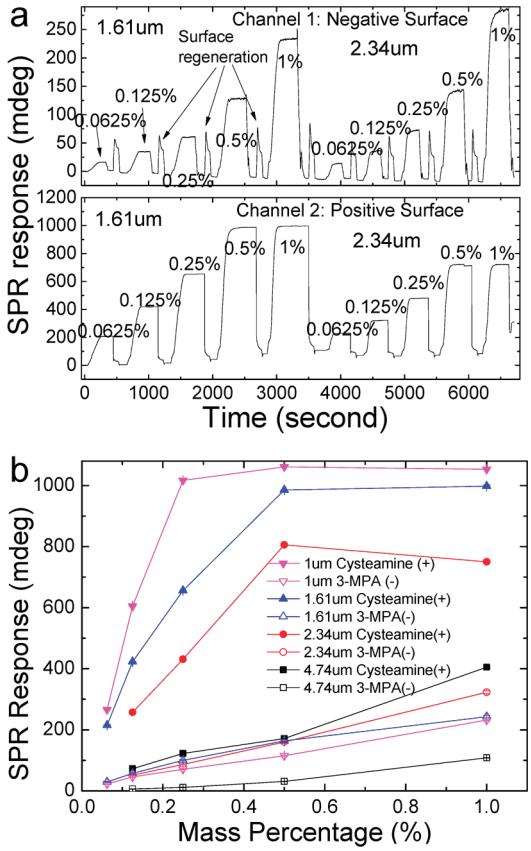

Figure 4. Particle concentration effect. (a) SPR response during the injection of silica particles with different concentrations and sizes for both positively and negatively charged surfaces. The small spikes between injections are caused by surface regeneration. (b) SPR responses versus particle concentration. Note that the error bars due to SPR noise are small.

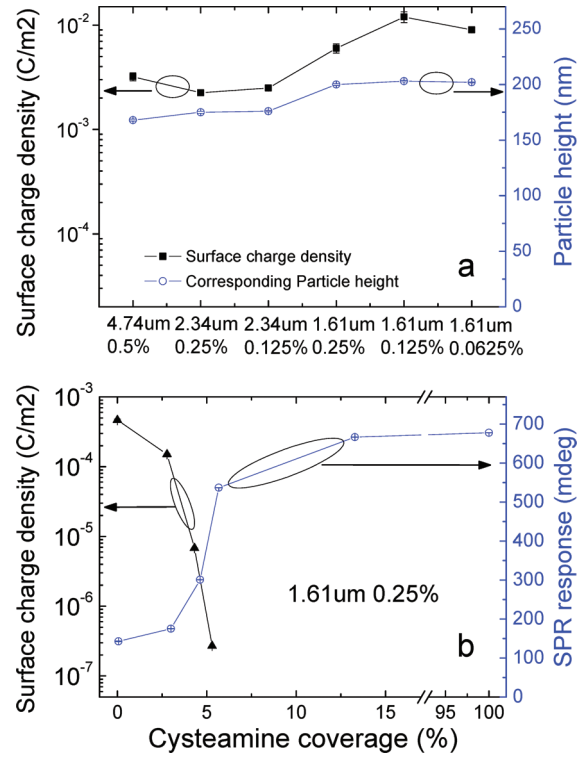

Figure 5. (a) Surface charge density of 3-MPA-modified surface determined by the SPR method. (b) Surface charge density (left axis) and corresponding SPR response (right axis) versus cysteamine surface coverage.

extracted the SPR angular shift as a function of concentration for particles with different sizes and surfaces with negative (3-MPA) and positive (cysteamine·HCl) charges (Figure 4b).

For the positively charged surface, the SPR response is proportional to the particle concentration below 0.25%, but the signal begins to saturate when the concentration is greater than 0.5% (see Figure 4a). This saturation corresponds to the formation of full monolayer coverage of particles. Further increasing the particle concentration can only result in the formation of second or multiple layers of the particles on the surface, which does not contribute to the SPR response due to limited penetration length of the evanescent field created by SPR. This means that to study a highly positively charged surface with negatively charged particles, one should use low concentration particles so as to avoid the saturation that limits the dynamic range. On the basis of these observations, we conclude that 1.61 and 2.34 μm particles at 0.25% or 0.125% are the best for measuring the surface charge density using the SPR method.

Surface Charge Density of 3-MPA-Modified Surface. We now turn to the determination of surface charge density using 3-MPA-modified surface as an example. For 0.25% 1.61 μm particle, the equilibrium height is ~200 nm, according to Figure 1b. Using this height and eqs 1−3, the surface charge density was found to be -6 ± 0.5 mC/m^2. We also performed the measurements using 1.61 μm particles at 0.125% and 0.0625% and obtained similar equilibrium heights and surface charge densities as shown in Figure 5a. Figure 5a also plots particle heights and surface charge densities for 2.34 and 4.74 μm diameter particles at different particle concentrations. As compared to 1.61 μm particles, the heights are somewhat smaller, and the corresponding surface charge densities of 2.34 and 4.74 μm particles are about -2.25 ± 0.13 and -3.2 ± 0.28 mC/m^2, respectively. This discrepancy is likely due to the greater effect of Brownian motion in the small particles, which is not included in eqs 1−3. In other words, the surface charge density obtained using 1.61 μm particles overestimates the actual surface charge density.

If we assume that the Au surface is fully covered with 3-MPA, which is reasonable because we inject 3-MPA for 240 s until the SPR signal saturated, then the surface density of 3-MPA, according to the STM study reported in literature,[23] is ~10^{19} m^{-2}. The pH of the acetate buffer is 5.0, and the pK_a of COOH$^-$-functionalized self-assembled monolayer on Au surface is 7.4.[24] Using these numbers and the relation pH = pK_a + log([A$^-$])/([HA]), we find that the surface charge density is −6.4 mC/m^2, which is in good agreement with the values determined using the present method. However, we point out that different methods have been applied to measure the pK_a of 3-MPA monolayer, and the reported values vary between 5.2 and 8.[25,26] Because pK_a is a logarithmic of the charge density, determining pK_a from charge density measurement is more accurate than the titration measurements.

(22) Dove, P. M.; Craven, C. M. *Geochim. Cosmochim. Acta* **2005**, *69*, 4963–4970.
(23) Giz, M. J.; Duong, B.; Tao, N. J. *J. Electroanal. Chem.* **1999**, *465*, 72–79.
(24) Fears, K. P.; Creager, S. E.; Latour, R. A. *Langmuir* **2008**, *24*, 837–843.
(25) Zhao, J. W.; Luo, L. Q.; Yang, X. R.; Wang, E. K.; Dong, S. J. *Electroanalysis* **1999**, *11*, 1108–1111.
(26) Kim, K.; Kwak, J. *J. Electroanal. Chem.* **2001**, *512*, 83–91.

Surface Charge Density Measurement at Different Cysteamine Coverages. To further demonstrate the method, we prepared sensor surfaces with different charge densities by varying cysteamine surface coverage. This was achieved by injecting low concentration (10 μM) cysteamine·HCl solution into the cell and exposing it to the Au film for 4, 5, 7, 10, and 240 s. The corresponding surface coverage values of cysteamine as determined from the SPR angular shifts were 2.78%, 4.31%, 5.3%, 12.5%, and 100%, respectively. As a reference, we also measured the surface charge density of bare Au and found that the Au film was slightly negatively charged under the experimental condition (Figure 5b). Increasing cysteamine coverage, the negatively charged Au surface was first neutralized by cysteamine and turned into positively charged when cysteamine coverage reached 5.3%. Further increasing the coverage over 12.5%, the negatively charged particles were attracted to the positively charged surface and form a complete layer, which led to the saturation of the SPR signal to a fixed value.

Error Analysis. The error in the measured surface charge density (σ) due to the noise in the measured SPR angular shift can be estimated from Figure 1c. According to Figure 1c, the surface charge density is related to the SPR response by $\ln \sigma = k \ln \theta$, within a wide range of surface charge densities, where k is the constant. The error in the surface charge density, $\delta\sigma$, is related to the error in the SPR signal, $\delta\theta$, by $\delta\sigma/\sigma = k\delta\theta/\theta$. For 1.61 μm particles at 0.25%, $k = -5.85$. The limit of detection of the SPR equipment is ~0.1 mdeg. On the basis of these parameters, the error is ~0.6% for high surface charge densities (10^{-2} C/cm^2) and ~0.1% for low surface charge densities (10^{-7} C/cm^2). Note that the error is smaller for lower surface charge densities, which can be understood on the basis of Figure 1a and b. According to Figure 1a, at lower surface charge densities, the particles are closer to the surface due to smaller repulsive forces between the particles and the surface. If the particles are closer to the surface, the SPR signal, according to Figure 1b, is more sensitive to the particle height due to the exponential decay of the evanescent field.

The error in the measured surface charge density due to noise in the SPR signal is quite small according to the analysis described above. According to eq 1, uncertainties in other parameters, including the particle size, particle concentration, and buffer concentration (via Debye length κ^{-1}), will also affect the accuracy of the surface charge density determined with the present method. The most significant contribution is the particle size, which has a standard deviation of 10−15%, corresponding to a maximum of 20−30% error in the surface charge density if the measurement is based on a single particle. The error will decrease if the measurement is based on a large number of particles. For example, if 1000 4.74 μm particles are used, the error drops to 3% based on a numerical simulation. Furthermore, more monodisperse particles (e.g., 2%) are commercially available, which can further increase the accuracy. Finally, we point out that unlike the random noise in the SPR signal, the particle size, particle concentration, and buffer concentration can be calibrated using the same SPR setup (via, e.g., the second channel).

CONCLUSION

SPR response is extremely sensitive to the vertical position of an objective over a SPR sensor surface. This unique feature can be used to accurately measure the equilibrium height of a particle over the surface. If the particle and surface are charged, then the equilibrium height is determined by the balance between gravity and electrostatic force on the particle. Both numerical simulations and experiments carried out in this work show a simple relation between the surface charge density and SPR response, which leads to a sensitive method to determine surface charge density. The sensitivity of the method depends on the particle size and concentration. Smaller particles are, in general, more sensitive than larger particles. However, if the particles are smaller than ~1 μm, then Brownian motion becomes important, which changes the relatively simple relation between SPR response and surface charge density. Higher particle concentrations are also more sensitive, but the upper limit is determined by the full coverage of the surface with particles. The particles demonstrated in this work were negatively charged silica particles, which acted as probes and amplifiers for sensitive detection of surface charge density. Other micro- and nano-objects, insulating, semiconducting, or metallic, may also be used as probes, as long as their optical properties are different from those of the buffer solution. Finally, we point out that this method can, in principle, determine the charge of micro- and nanoscale objects if the surface charge of the sensor is known or calibrated.

ACKNOWLEDGMENT

This work has been supported by the NSF (CHM-0554786).

SUPPORTING INFORMATION AVAILABLE

Particle−surface interactions' equations and their derivations, SPR-particle height simulations, particle size effect, simulated SPR profiles with and without particles, and zeta-potential measurements. This material is available free of charge via the Internet at http://pubs.acs.org.

Received for review August 12, 2009. Accepted November 9, 2009.

AC901816Z